



Uncertainty of Predictions of Embankment Dam Breach Parameters

Tony L. Wahl¹

Abstract: Risk assessment studies considering the failure of embankment dams often require the prediction of basic geometric and temporal parameters of a breach, or the estimation of peak breach outflows. Many of the relations most commonly used to make these predictions were developed from statistical analyses of data collected from historic dam failures. The prediction uncertainties of these methods are widely recognized to be very large, but have never been specifically quantified. This paper presents an analysis of the uncertainty of many of these breach parameter and peak flow prediction methods. Application of the methods and the uncertainty analysis are illustrated through a case study of a risk assessment recently performed by the Bureau of Reclamation for a large embankment dam in North Dakota.

DOI: 10.1061/(ASCE)0733-9429(2004)130:5(389)

CE Database subject headings: Dam failure; Uncertainty analysis; Peak flow; Erosion; Dams, embankment; Risk management.

Introduction

Risk assessment studies considering the failure of embankment dams often make use of breach parameter prediction methods that have been developed from analysis of historic dam failures. Similarly, predictions of peak breach outflow can also be made using relations developed from case study data. This paper presents an analysis of the uncertainty of many of these breach parameter and peak flow prediction methods, making use of a previously compiled database (Wahl 1998) of 108 dam failures. Subsets of this database were used by other investigators to develop many of the relations examined.

The paper begins with a brief discussion of breach parameters and prediction methods. The uncertainty analysis of the various methods is presented next, and finally, a case study is offered to illustrate the application of several breach parameter prediction methods and the uncertainty analysis to a risk assessment recently performed by the Bureau of Reclamation for a large embankment dam in North Dakota.

Breach Parameters

Dam-break flood routing models [e.g., *DAMBRK* (Fread 1984) and *FLDWAV* (Fread 1993)] simulate the outflow from a reservoir and through the downstream valley resulting from a developing breach in a dam. These models focus their computational effort on the routing of the breach outflow hydrograph. The development of the breach is not simulated in any physical sense, but

rather is idealized as a parametric process, defined by the shape of the breach, its final size, and the time required for its development (often called the failure time). Breaches in embankment dams are usually assumed to be trapezoidal, so the shape and size of the breach are defined by a base width and side slope angle, or more simply by an average breach width.

The failure time is a critical parameter affecting the outflow hydrograph and the consequences of dam failure, especially when populations at risk are located close to a dam so that available warning and evacuation time dramatically affect loss of life. For the purpose of routing a dam-break flood wave, breach development begins when a breach has reached the point at which the volume of the reservoir is compromised and failure becomes imminent. During the breach development phase, outflow from the dam increases rapidly. The breach development time ends when the breach reaches its final size; in some cases, this may also correspond to the time of peak outflow through the breach, but for relatively small reservoirs the peak outflow may occur before the breach is fully developed. The breach development time as described above is the parameter intended to be predicted by most failure time prediction equations.

The breach development time does not include the potentially long preceding period described as the breach initiation phase (Wahl 1998), which can also be important when considering available warning and evacuation time. This is the first phase of an overtopping failure, during which flow overtops a dam and may erode the downstream face, but does not create a breach through the dam that compromises the reservoir volume. If the overtopping flow were quickly stopped during the breach initiation phase, the reservoir would not fail. In an overtopping failure, the length of the breach initiation phase is important, because breach initiation can potentially be observed and may thus trigger warning and evacuation. Unfortunately, there are few tools presently available for predicting the length of the breach initiation phase.

During a seepage-erosion (piping) failure, the delineation between breach initiation and breach development phases is less apparent. In some cases, seepage-erosion failures can take a great deal of time to develop. In contrast to the overtopping case, the

¹Hydraulic Engineer, U.S. Dept. of the Interior, Bureau of Reclamation, Water Resources Research Laboratory D-8560, P.O. Box 25007, Denver, CO 80225-0007. E-mail: twahl@do.usbr.gov

Note. Discussion open until October 1, 2004. Separate discussions must be submitted for individual papers. To extend the closing date by one month, a written request must be filed with the ASCE Managing Editor. The manuscript for this paper was submitted for review and possible publication on June 25, 2002; approved on September 25, 2003. This paper is part of the *Journal of Hydraulic Engineering*, Vol. 130, No. 5, May 1, 2004. ©ASCE, ISSN 0733-9429/2004/5-389-397/\$18.00.

loading that causes a seepage-erosion failure cannot normally be removed quickly, and the process does not take place in full view, except that the outflow from a developing pipe can be observed and measured. One useful way to view seepage-erosion failures is to consider three possible conditions:

1. Normal seepage outflow, with clear water and low flow rates;
2. Initiation of a seepage-erosion failure with cloudy seepage water that indicates a developing pipe, but flow rates are still low and not rapidly increasing. Corrective actions might still be possible that would heal the developing pipe and prevent failure.
3. Active development phase of a seepage-erosion failure in which erosion is dramatic and flow rates are rapidly increasing. Failure cannot be prevented.

Only the length of the last phase is important when determining the breach hydrograph from a dam, but both the breach initiation and breach development phases may be important when considering warning and evacuation time. Again, as with the overtopping failure, there are few tools available for estimating the length of the breach initiation phase.

Predicting Breach Parameters

To carry out a dam-break flood routing simulation, breach parameters must be estimated and provided as inputs to the dam-break and flood routing simulation model. Several methods are available for estimating breach parameters; a summary of the available methods was provided by Wahl (1998). The simplest methods (Johnson and Illes 1976; Singh and Snorrason 1984; Bureau of Reclamation 1988) predict the average breach width as a linear function of either the height of the dam or the depth of water stored behind the dam at the time of failure. Slightly more sophisticated methods predict more specific breach parameters, such as breach base width, side slope angles, and failure time, as functions of one or more dam and reservoir properties, such as storage volume, depth of water at failure, depth of breach, etc. All of these methods are based on regression analyses of data collected from actual dam failures. The database of dam failures used to develop these relations is relatively lacking in data from failures of large dams, with about 75% of the cases having a height less than 15 m (Wahl 1998).

Physically based simulation models are available to aid in the prediction of breach parameters. None are widely used at this time, but the most notable is the National Weather Service (NWS)-BREACH model (Fread 1988). These models simulate the hydraulic and erosion processes associated with flow over an overtopping dam or through a developing piping channel. Through such a simulation, an estimate of the breach parameters may be developed for use in a dam-break flood routing model, or the outflow hydrograph at the dam can be predicted directly. The primary weakness of the NWS-BREACH model, and other similar models, is the fact that they do not adequately model the headcut-type erosion processes that dominate the breaching of cohesive-soil embankments (e.g., Hanson et al. 2002). Recent work by the Agricultural Research Service (e.g., Temple and Moore 1997) on headcut erosion in earth spillways has shown that headcut erosion is best modeled with methods based on energy dissipation.

Predicting Peak Outflow

In addition to the prediction of breach parameters, many investigators have proposed simplified methods for predicting peak out-

flow from a breached dam. These methods are used for reconnaissance-level work and for checking the reasonability of dam-break outflow hydrographs developed from estimated breach parameters. This paper considers the relations by Kirkpatrick (1977), SCS (1981), Hagen (1982), Bureau of Reclamation (1982), MacDonald and Langridge-Monopolis (1984), Singh and Snorrason (1984), Costa (1985), Evans (1986), Froehlich (1995b), and Walder and O'Connor (1997).

All of these methods, except Walder and O'Connor, are straightforward regression relations that predict peak outflow as a function of various dam and/or reservoir parameters, with the relations developed from analyses of case study data from real dam failures. In contrast, Walder and O'Connor's method is based upon an analysis of numerical simulations of idealized cases spanning a range of dam and reservoir configurations and erosion scenarios. An important parameter in their method is an assumed vertical erosion rate of the breach; for reconnaissance-level estimating purposes, they suggest that a range of reasonable values is 10 to 100 m/h, based on an analysis of case study data. The method makes a distinction between so-called large-reservoir/fast-erosion and small-reservoir/slow-erosion cases. In large-reservoir cases, the peak outflow occurs when the breach reaches its maximum depth, before there has been any significant drawdown of the reservoir. In this case, the peak outflow is insensitive to the erosion rate. In the small-reservoir case, there is a significant drawdown of the reservoir as the breach develops, and thus the peak outflow occurs before the breach erodes to its maximum depth. Peak outflows for small-reservoir cases are dependent on the vertical erosion rate and can be dramatically smaller than for large-reservoir cases. The determination of whether a specific situation is a large- or small-reservoir case is based on a dimensionless parameter incorporating the embankment erosion rate, reservoir size, and change in reservoir level during the failure. Thus, so-called large-reservoir/fast-erosion cases can occur even with what might be considered "small" reservoirs and vice versa. This refinement is not present in any of the other peak flow prediction methods.

Developing Uncertainty Estimates

In a typical risk assessment study, a variety of loading and failure scenarios are analyzed. This allows the study to incorporate variability in antecedent conditions and the probabilities associated with different loading conditions and failure scenarios. The uncertainty of key parameters (e.g., material properties) is sometimes considered by creating scenarios in which analyses are carried out with different parameter values and a probability of occurrence assigned to each value of the parameter. Although the uncertainty of breach parameter predictions is often very large, there have previously been no quantitative assessments of this uncertainty, and thus breach parameter uncertainty has not been incorporated into most risk assessment studies.

It is worthwhile to consider breach parameter prediction uncertainty in the risk assessment process because the uncertainty of breach parameter predictions is likely to be significantly greater than all other factors, and could thus dramatically influence the outcome. For example, Wahl (1998) used many of the available relations to predict breach parameters for 108 documented case studies and plot the predictions against the observed values. Prediction errors of $\pm 75\%$ were not uncommon for breach width, and prediction errors for failure time often exceeded one order of magnitude. Most relations used to predict failure time are conser-

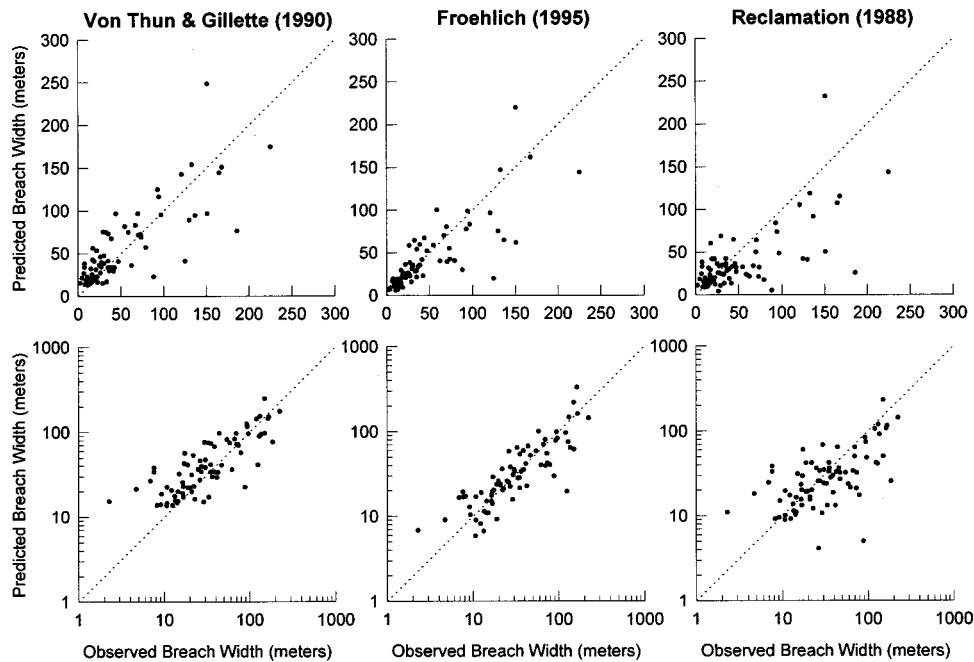


Fig. 1. Predicted and observed breach widths (Wahl 1998), plotted arithmetically (top) and on logarithmic scales (bottom)

vatively designed to underpredict the reported time more often than they overpredict, but overprediction errors of more than one-half of an order of magnitude did occur several times.

The first question that must be addressed in an uncertainty analysis of breach parameter predictions is how to express the results. The case study datasets used to develop most breach parameter prediction equations include data from a wide range of dam sizes, and thus, regressions in log-log space have been commonly used. Fig. 1 shows the observed and predicted breach widths as computed by Wahl (1998) in both arithmetically scaled and log-log plots. In the arithmetic plots, it would be difficult to draw in upper and lower bound lines to define an uncertainty band. In the log-log plots, data are scattered approximately evenly above and below the lines of perfect prediction, suggesting that uncertainties would best be expressed as a number of log cycles on either side of the predicted value. This is the approach taken in the analysis that follows.

The other notable feature of the plots in Fig. 1 is the presence of some significant outliers. Possible sources of these outliers include the variable quality of the case study parameter observations being used to test the predictions and the potential for misapplication of some of the prediction equations in the analysis described here due to lack of detailed firsthand knowledge of each case study situation. Such problems should not affect a careful future application of these prediction equations to a specific case, and we do not wish for them to affect the present analysis of the uncertainties of the methods themselves. Admittedly, much of the scatter and the appearance of outliers are probably due to the inherent variability of the data caused by the variety of factors that influence dam breach mechanics, and this variability should be preserved as we analyze the uncertainties of the prediction equations. To exclude the truly anomalous data (the statistical outliers) and retain the characteristic variability, an objective outlier exclusion algorithm was applied (Rousseeuw 1998). The selected algorithm has the advantage that its performance is itself insensitive to the presence of the outliers, which overcomes a common problem encountered when attempting to exclude outliers.

The uncertainty analysis was performed using the database presented in Wahl (1998), with data on 108 case studies of actual embankment dam failures, collected from numerous sources in the literature. The majority of the available breach parameter and peak flow prediction equations were applied to this database of dam failures, and the predicted values were compared to the observed values. Computation of breach parameters or peak flows was straightforward in most cases. A notable exception was the peak flow prediction method of Walder and O'Connor (1997), which requires that the reservoir be classified as a large- or small-reservoir case. In addition, in the case of the small-reservoir situation, an average vertical erosion rate of the breach must be estimated. The Walder and O'Connor method was applied only to those dams that could be clearly identified as large-reservoir (where peak outflow is insensitive to the vertical erosion rate) or small-reservoir with an associated estimate of the vertical erosion rate obtained from observed breach heights and failure times. Two other facts should be noted:

1. No prediction equation could be applied to all 108 dam failure cases, due to the lack of required input data for the specific equation or the lack of an observed value of the parameter of interest. Most of the breach width equations could be tested against about 70 to 80 cases, the failure time equations against 30 to 40 cases, and the peak flow prediction equations against about 30 to 40 cases.
2. The testing made use of the same data used to originally develop many of the equations (since the 108-dam database was compiled from these and other sources), but each equation was also tested against additional cases, the number varying depending on the method. This should provide a fair indication of the ability of each equation to predict breach parameters for future dam failures. (It is difficult to say exactly how many additional cases were analyzed for each method, since the exact number of failures used to develop each method is not indicated clearly in literature for all methods, and some are based on a combination of statistical analysis of case studies and physically based theory.)

A step-by-step description of the uncertainty analysis method follows:

1. Plot predicted versus observed values on log–log scales.
2. Compute individual prediction errors in terms of the number of log cycles separating the predicted and observed value, $e_i = \log_{10}(\hat{x}) - \log_{10}(x) = \log_{10}(\hat{x}/x)$, where e_i is the prediction error, \hat{x} is the predicted value, and x is the observed value.
3. Apply the outlier-exclusion algorithm to the series of prediction errors computed in Step 2. The algorithm is described by Rousseeuw (1998).
 - Determine T , the median of the e_i values. T is the estimator of location.
 - Compute the absolute values of the deviations from the median, and determine the median of these absolute deviations (MAD).
 - Compute an estimator of scale, $S_{MAD} = 1.483 * (\text{MAD})$. The 1.483 factor makes S_{MAD} comparable to the standard deviation, which is the usual scale parameter of a normal distribution.
 - Use S_{MAD} and T to compute a Z score for each observation, $Z_i = (e_i - T) / S_{MAD}$, where the e_i 's are the observed prediction errors, expressed as a number of log cycles.
 - Reject any observations for which $|Z_i| > 2.5$.
 - If the samples are from a perfect normal distribution, this method rejects at the 98.7% probability level. Testing showed that application to normally distributed data would lead to an average 3.9% reduction of the standard deviation.
4. Compute the mean, \bar{e} , and the standard deviation, S_e , of the remaining prediction errors. If the mean value is negative, it indicates that the prediction equation underestimated the observed values, and if positive the equation overestimated the observed values. Significant over or underestimation should be expected, since many of the breach parameter prediction equations are intended to be conservative or provide envelope estimates, e.g., maximum reasonable breach width, fastest possible failure time, etc.
5. Using the values of \bar{e} and S_e , one can express a confidence band around the predicted value of a parameter as $\{\hat{x} \cdot 10^{-\bar{e}-2S_e}, \hat{x} \cdot 10^{-\bar{e}+2S_e}\}$, where \hat{x} is the predicted value. The use of $\pm 2S_e$ approximately yields a 95% confidence band.

Table 1 summarizes the results. The first two columns identify the method being analyzed, the next two columns show the number of case studies used to test the method, and the next two columns give the prediction error and the width of the uncertainty band. The last column shows the range of the prediction interval around a hypothetical predicted value of 1.0. The values in this column can be used as multipliers to obtain the prediction interval for a specific case.

Although the detailed data are not shown in Table 1, prediction errors and uncertainties also were determined prior to applying the outlier exclusion algorithm to determine its effect. Outlier exclusion reduced the values of S_e by at least 5% up to about 20% in most cases. Since this exceeds the 3.9% reduction one would expect when applying the algorithm to a normally distributed dataset, it suggests that true outliers were excluded rather than just occasional extreme values that one would expect in normally distributed data. The use of outlier exclusion did not materially change the results of the study (i.e., the same methods had the lowest uncertainty before and after outlier exclusion). One notable fact is that the outlier exclusion algorithm reduced S_e by 30

to 60% for two of the breach width equations (Bureau of Reclamation 1988; Von Thun and Gillette 1990) and four of the peak flow equations [Kirkpatrick 1977; SCS 1981; Bureau of Reclamation 1982; Singh and Snorrason 1984 (the first of the two equations shown in Table 1)]. All of these prediction equations are based solely on the dam height or water depth above the breach invert, suggesting that dam height by itself is a poor predictor for breach width or peak outflow.

Summary of Uncertainty Analysis Results

The four methods for predicting breach width (or volume of material eroded, from which breach width can be estimated) all had absolute mean prediction errors less than one-tenth of an order of magnitude, indicating that on average their predictions are on target. The uncertainty bands were similar (± 0.3 to ± 0.4 log cycles) for all of the equations except the MacDonald and Langridge-Monopolis equation, which had an uncertainty of ± 0.82 log cycles.

The five methods for predicting failure time all underpredict the failure time on average, by amounts ranging from about one-fifth to two-thirds of an order of magnitude. This is consistent with the previous observation that these equations are designed to conservatively predict fast breaches, which will cause large peak outflows. The uncertainty bands on all of the failure time equations are very large, ranging from about ± 0.6 to ± 1 order of magnitude, with the Froehlich (1995a) equation having the smallest uncertainty.

Most of the peak flow prediction equations tend to overpredict observed peak flows, with most of the “envelope” equations overpredicting by about two-thirds to three-quarters of an order of magnitude. The uncertainty bands on the peak flow prediction equations are about ± 0.5 to ± 1 order of magnitude, except the Froehlich (1995b) relation which has an uncertainty of ± 0.32 order of magnitude. In fact, the Froehlich equation has both the lowest prediction error and smallest uncertainty of all the peak flow prediction equations.

Application

To illustrate the application of the uncertainty analysis results, a case study is presented. In January 2001 the Bureau of Reclamation conducted a risk assessment study for a large embankment dam in North Dakota (Fig. 2). Two potential failure modes were considered: (1) Seepage erosion and piping through foundation materials, and (2) seepage erosion and piping through embankment materials. No distinction between the two failure modes was made in the breach parameter analysis, since most methods used to predict breach parameters lack the refinement needed to consider differences in breach morphology for such similar failure modes. Breach parameters were predicted using most of the methods discussed earlier in this paper, and also by modeling with the NWS-BREACH model.

The potential for failure and the downstream consequences from failure increase significantly at higher reservoir levels, although the likelihood of occurrence of high reservoir levels is low. The reservoir rarely exceeds its top-of-joint-use elevation (the water surface elevation corresponding to the maximum amount of storage allocated to joint use, i.e., flood control and

Table 1. Uncertainty Estimates for Breach Parameter and Peak Flow Prediction Equations

| Reference | Equation | Number of case studies | | Mean prediction error (log cycles) | Width of uncertainty band, $\pm 2S_e$ (log cycles) | Prediction interval around hypothetical predicted value of 1.0 |
|--|--|--------------------------|-------------------------|------------------------------------|--|--|
| | | Before outlier exclusion | After outlier exclusion | | | |
| Breach width equations | | | | | | |
| Bureau of Reclamation (1988) | $B_{avg} = 3h_w$ | 80 | 70 | -0.09 | ± 0.43 | 0.45–3.3 |
| MacDonald and Langridge-Monopolis (1984) | $V_{er} = 0.0261(V_w h_w)^{0.769}$ earthfills $V_{er} = 0.00348(V_w h_w)^{0.852}$ nonearthfills (e.g., rockfills) | 60 | 58 | -0.01 | ± 0.82 | 0.15–6.8 |
| Von Thun and Gillette (1990) | $B_{avg} = 2.5h_w + C_b$ | 78 | 70 | +0.09 | ± 0.35 | 0.37–1.8 |
| Froehlich (1995a) | $B_{avg} = 0.1803K_o V_w^{0.32} h_b^{0.19}$ | 77 | 75 | +0.01 | ± 0.39 | 0.40–2.4 |
| Failure time equations | | | | | | |
| MacDonald and Langridge-Monopolis (1984) | $t_f = 0.0179V_{er}^{0.364}$ | 37 | 35 | -0.21 | ± 0.83 | 0.24–11 |
| Von Thun and Gillette (1990) | $t_f = 0.015h_w$ highly erodible $t_f = 0.020h_w + 0.25$ erosion resistant | 36 | 34 | -0.64 | ± 0.95 | 0.49–40 |
| Von Thun and Gillette (1990) | $t_f = B_{avg}/(4h_w)$ erosion resistant $t_f = B_{avg}/(4h_w + 61)$ highly erodible | 36 | 35 | -0.38 | ± 0.84 | 0.35–17 |
| Froehlich (1995a) | $t_f = 0.00254(V_w)^{0.53} h_b^{-0.9}$ | 34 | 33 | -0.22 | ± 0.64 | 0.38–7.3 |
| Bureau of Reclamation (1988) | $t_f = 0.011(B_{avg})$ | 40 | 39 | -0.40 | ± 1.02 | 0.24–27 |
| Peak flow equations | | | | | | |
| Kirkpatrick (1977) | $Q_p = 1.268(h_w + 0.3)^{2.5}$ | 38 | 34 | -0.14 | ± 0.69 | 0.28–6.8 |
| SCS (1981) | $Q_p = 16.6(h_w)^{1.85}$ | 38 | 32 | +0.13 | ± 0.50 | 0.23–2.4 |
| Hagen (1982) | $Q_p = 0.54(S \cdot h_d)^{0.5}$ | 31 | 30 | +0.43 | ± 0.75 | 0.07–2.1 |
| Bureau of Reclamation (1982) | $Q_p = 19.1(h_w)^{1.85}$ envelope eq. | 38 | 32 | +0.19 | ± 0.50 | 0.20–2.1 |
| Singh and Snorrason (1984) | $Q_p = 13.4(h_d)^{1.89}$ | 38 | 28 | +0.19 | ± 0.46 | 0.23–1.9 |
| Singh and Snorrason (1984) | $Q_p = 1.776(S)^{0.47}$ | 35 | 34 | +0.17 | ± 0.90 | 0.08–5.4 |
| MacDonald and Langridge-Monopolis (1984) | $Q_p = 1.154(V_w h_w)^{0.412}$ | 37 | 36 | +0.13 | ± 0.70 | 0.15–3.7 |
| MacDonald and Langridge-Monopolis (1984) | $Q_p = 3.85(V_w h_w)^{0.411}$ envelope eq. | 37 | 36 | +0.64 | ± 0.70 | 0.05–1.1 |
| Costa (1985) | $Q_p = 1.122(S)^{0.57}$ | 35 | 35 | +0.69 | ± 1.02 | 0.02–2.1 |
| Costa (1985) | $Q_p = 0.981(S \cdot h_d)^{0.42}$ | 31 | 30 | +0.05 | ± 0.72 | 0.17–4.7 |
| Costa (1985) | $Q_p = 2.634(S \cdot h_d)^{0.44}$ | 31 | 30 | +0.64 | ± 0.72 | 0.04–1.22 |
| Evans (1986) | $Q_p = 0.72(V_w)^{0.53}$ | 39 | 39 | +0.29 | ± 0.93 | 0.06–4.4 |
| Froehlich (1995b) | $Q_p = 0.607(V_w^{0.295} h_w^{1.24})$ | 32 | 31 | -0.04 | ± 0.32 | 0.53–2.3 |
| Walder and O'Connor (1997) | Q_p estimated by computational and graphical method using relative erodibility of dam and volume of reservoir | 22 | 21 | +0.13 | ± 0.68 | 0.16–3.6 |

Note: All equations use metric units (m, m³, m³/s). Failure times are computed in hours. Where multiple equations are shown for application to different types of dams (e.g., earthfill versus rockfill), a single prediction uncertainty was determined, with the *set* of equations considered as a single algorithm.

conservation purposes), and has never exceeded an elevation of 440.7 m. Four potential reservoir water surface elevations at failure were considered in the study:

- Top-of-joint-use, elevation: 436.67 m, reservoir capacity of about 45.6×10^6 m³,
- Elevation 438.91 m, reservoir capacity of about 105×10^6 m³,
- Top-of-flood-space (the design maximum reservoir level reached during the temporary storage of flood runoff), elevation 443.18 m, reservoir capacity of about 273×10^6 m³, and
- Maximum design water surface, elevation: 446.32 m, storage of about 469×10^6 m³.

For illustration purposes, only the results from the top-of-joint-use and top-of-flood-space cases are presented here.

Dam Description

The case study dam is located a few kilometers upstream from a city with a population of about 15,000. It was constructed by the Bureau of Reclamation in the early 1950's. The dam is operated by Reclamation to provide flood control, municipal water supply, and recreational and wildlife benefits.

The dam is a zoned-earth fill with a height of 24.7 m above the original streambed. The crest length is 432 m at an elevation of 448.36 m and the crest width is 9.14 m. The design includes a central compacted zone 1 of impervious material, and upstream and downstream zone 2 of sand and gravel, shown in Fig. 3. The abutments are composed of Pierre Shale capped with glacial till. The main portion of the dam is founded on a thick section of



Fig. 2. Aerial photo of the dam and reservoir considered in the case study application

alluvial deposits. Beneath the dam, a cutoff trench was excavated to the shale on both abutments, but between the abutments, foundation excavation extended to a maximum depth of 7.6 m, and did not provide a positive cutoff of the thick alluvium. The alluvium beneath the dam is more than 37 m thick in the channel area.

There is a toe drain within the downstream embankment near the foundation level, and a wide embankment section to help control seepage beneath the dam, since a positive cutoff was not constructed. Based on observations of increasing pressures in the foundation during high reservoir elevations and significant boil activity downstream from the dam, eight relief wells were installed along the downstream toe in 1995 and 1996. To increase the seepage protection, a filter blanket was constructed in low areas downstream from the dam in 1998.

Results—Breach Parameter Estimates

Predictions were made for average breach width, volume of eroded material, and failure time. Side slope angles were not predicted because equations for predicting breach side slope angles are rare in literature; Froehlich (1987) offered an equation, but in his later paper (1995a), he suggested simply assuming side slopes of 0.9:1 (horizontal:vertical) for piping failures. Von Thun and Gillette (1990) suggested using side slopes of 1:1, except for cases of dams with very thick zones of cohesive materials where side slopes of 0.5:1 or 0.33:1 might be appropriate.

After computing breach parameters using the many available equations, the results were reviewed and judgment applied to develop a single predicted value and an uncertainty band to be provided to the risk assessment study team. These recommended values are shown at the bottom of each column in the tables that follow.

Breach Width

Predictions of average breach width are summarized in Table 2. Table 2 also lists the predictions of the volume of eroded embankment material made using the MacDonald and Langridge-Monopolis equation, and the corresponding estimate of average breach width.

The uncertainty analysis described earlier showed that the Reclamation equation tends to underestimate the observed breach width, so it is not surprising that it yielded the smallest values. The Von Thun and Gillette equation and the Froehlich equation produced comparable results for the top-of-joint-use scenario, in which reservoir storage is relatively small. For the top-of-flood-space scenario, the Froehlich equation predicts significantly larger breach widths. This is not surprising, since the Froehlich equation relates breach width to an exponential function of both the reservoir storage and reservoir depth. The Von Thun and Gillette equation accounts for reservoir storage only through the C_b offset parameter, but C_b is a constant for all reservoirs larger than $12.3 \times 10^6 \text{ m}^3$, as was the case for both scenarios.

Using the MacDonald and Langridge-Monopolis equation, the estimate of eroded embankment volume and associated breach width for the top-of-joint-use scenario is also comparable to the other equations. However, for the top-of-flood-space scenario, the prediction is much larger than any of the other equations, and in fact is unreasonable because it exceeds the dimensions of the dam.

The prediction intervals developed through the uncertainty analysis are sobering for the analyst wishing to obtain a definitive result, as the ranges vary from small notches through the dam to a complete washout of the embankment. Even for the top-of-joint-use case, the upper bounds for the Froehlich equation and the Von Thun and Gillette equation are equivalent to about one-half of the length of the embankment.

Failure Time

Failure time predictions are summarized in Table 3. All of the equations indicate increasing failure times as the reservoir storage increases, except the second Von Thun and Gillette relation, which predicts a slight decrease in failure time for the top-of-flood-space scenario. For both Von Thun and Gillette relations, the dam was assumed to be in the erosion resistant category.

The predicted failure times exhibit wide variation, and the recommended values shown at the bottom of Table 3 are based on much judgment. The uncertainty analysis showed that all of the failure time equations tend to conservatively underestimate actual failure times, especially the Von Thun and Gillette and Reclamation equations. Thus, the recommended values are generally a compromise between the results obtained from the MacDonald

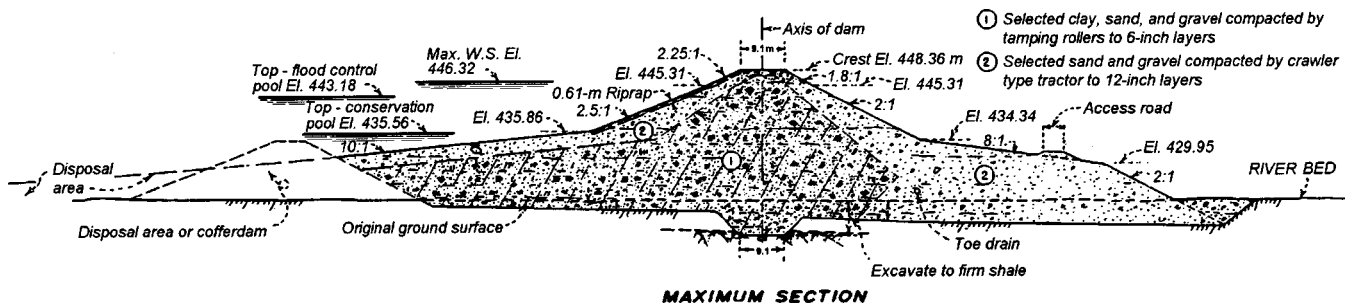


Fig. 3. Cross section through the case study dam

Table 2. Predictions of Average Breach Width

| Equation | Top of joint use, elevation of 436.68 m | | Top of flood space, elevation of 443.18 m | |
|--|---|-------------------------|---|-------------------------|
| | Predicted breach width (m) | 95% prediction interval | Predicted breach width (m) | 95% prediction interval |
| Bureau of Reclamation (1988) | 39.0 | 17.7–129 | 58.5 | 26.2–193 |
| Von Thun and Gillette (1990) | 87.5 | 32.3–157 | 104 | 38.4–187 |
| Froehlich (1995a) | 93.6 | 37.5–225 | 166 | 66.4–398 |
| MacDonald and Langridge-Monopolis (1984) | 146,000 | 22,200–991,000 | 787,000 | 118,000–5,350,000 |
| Volume of erosion (m ³) | | | | |
| Equivalent breach width (m) | 85.6 | 12.8–582 ^a | 462 ^a | 69.2–3140 ^a |
| Recommended values (m) | 90 | 35–180 | 165 | 60–400 |

^aExceeds actual embankment length.

and Langridge-Monopolis and Froehlich relations. Despite this fact, some very fast failures are documented in literature, and this possibility is reflected in the prediction intervals determined from the uncertainty analysis.

Results—Peak Outflow Estimates

Peak outflow estimates are shown in Table 4, sorted in order of increasing peak outflow for the top-of-joint-use scenario. The lowest peak flow predictions come from those equations that are based solely on dam height or depth of water in the reservoir. The highest peak flows are predicted by those equations that incorporate a significant dependence on reservoir storage. Some of the predicted peak flows and the upper bounds of the prediction limits would be the largest dam-break outflows ever recorded, exceeding the 65,000 m³/s peak outflow from the Teton Dam failure. (Storage in Teton Dam at failure was 356×10^6 m³). The length of the reservoir (about 48 km) may help to attenuate some of the large peak outflows predicted by the storage-sensitive equations, since there will be an appreciable routing effect in the reservoir itself that is probably not accounted for in the peak flow prediction equations.

The equation offered by Froehlich (1995b) clearly had the best prediction performance in the uncertainty analysis, and is thus highlighted in Table 4. This equation had the smallest mean prediction error and narrowest prediction interval by a significant margin.

The results for the Walder and O'Connor method are also highlighted. As discussed earlier, this is the only method that considers the differences between the so-called large-reservoir/fast-erosion and small-reservoir/slow-erosion cases. This dam proves to be a large-reservoir/fast-erosion case when analyzed by this method (regardless of the assumed vertical erosion rate of the breach—within reasonable limits), so the peak outflow will occur

when the breach reaches its maximum size, before significant drawdown of the reservoir has occurred. Despite the refinement of considering large- versus small-reservoir behavior, the Walder and O'Connor method was found to have uncertainty similar to most of the other peak flow prediction methods (about ± 0.75 log cycles). However, among the 22 case studies to which the method could be applied, only four proved to be large-reservoir/fast-erosion cases. Of these, the method overpredicted the peak outflow in three cases, and dramatically underpredicted in one case (Goose Creek Dam, South Carolina, failed 1916 by overtopping). Closer examination showed some contradictions in the data reported in literature for this case. On balance, it appears that the Walder and O'Connor method may provide reasonable estimates of the upper limit on peak outflow for large-reservoir/fast-erosion cases.

For this application, results from the Froehlich method were considered to be the best estimate of peak breach outflow, and the results from the Walder and O'Connor method provided an upper bound estimate.

NWS-BREACH Simulations

Several simulations runs were made using the NWS-BREACH model (Fread 1988). The model requires input data related to reservoir bathymetry, dam geometry, the tailwater channel, embankment materials, and initial conditions for the simulated piping failure.

The results of the simulations are very sensitive to the elevation at which the piping failure is assumed to develop. In all cases analyzed, the maximum outflow occurred just prior to the crest of the dam collapsing into the pipe; after the collapse of the crest, a large volume of material partially blocks the breach and the outflow becomes weir controlled until the material can be removed. Thus, the largest peak outflows and largest breach sizes are ob-

Table 3. Failure Time Predictions

| Equation | Top of joint use, elevation of 436.68 m | | Top of flood space, elevation of 443.18 m | |
|---|---|-------------------------|---|-------------------------|
| | Predicted failure time (h) | 95% prediction interval | Predicted failure time (h) | 95% prediction interval |
| MacDonald and Langridge-Monopolis (1984) | 1.36 | 0.33–14.9 | 2.45 ^a | 0.59–26.9 |
| Von Thun and Gillette (1990), $t_f = f(h_w)$ | 0.51 | 0.25–20.4 | 0.64 | 0.31–25.6 |
| Von Thun and Gillette (1990), $t_f = f(B, h_w)$ | 1.68 | 0.59–28.6 | 1.33 | 0.47–22.6 |
| Froehlich (1995a) | 1.63 | 0.62–11.9 | 4.19 | 1.59–30.6 |
| Bureau of Reclamation (1988) | 0.43 | 0.10–11.6 | 0.64 | 0.15–17.4 |
| Recommended values | 1.5 | 0.25–12 | 3.0 | 0.3–17 |

^aPredicted erosion volume exceeded total embankment volume; total embankment volume was used in the failure time equation.

Table 4. Predictions of Peak Breach Outflow

| Equation | Top of joint use, elevation of 436.68 m | | Top of flood space, elevation of 443.18 m | |
|---|--|-------------------------|--|-------------------------|
| | Predicted peak outflow (m ³ /s) | 95% prediction interval | Predicted peak outflow (m ³ /s) | 95% prediction interval |
| Kirkpatrick (1977) | 818 | 229–5,570 | 2,210 | 620–15,100 |
| SCS (1981) | 1,910 | 439–4,590 | 4,050 | 932–9,710 |
| Bureau of Reclamation (1982) (envelope) | 2,200 | 439–4,620 | 4,660 | 932–9,780 |
| Froehlich (1995b) | 2,660 | 1,410–6,110 | 7,440 | 3,940–17,100 |
| MacDonald/Langridge-Monopolis (1984) | 4,750 | 714–17,600 | 11,700 | 1,760–43,400 |
| Singh/Snorrason (1984), $Q_p = f(h_d)$ | 5,740 | 1,320–10,900 | 5,740 | 1,320–10,900 |
| Walder and O'Connor (1997) | 6,000 | 960–21,400 | 12,200 | 1,950–43,500 |
| Costa (1985), $Q_p = f(S * h_d)$ | 6,220 | 1,060–29,200 | 13,200 | 2,240–61,900 |
| Singh/Snorrason (1984), $Q_p = f(S)$ | 7,070 | 570–38,200 | 16,400 | 1,310–88,400 |
| Evans (1986) | 8,260 | 496–36,300 | 21,300 | 1,280–93,700 |
| MacDonald/Langridge-Monopolis (1984) (envelope) | 15,500 | 776–17,100 | 38,300 | 1,910–42,100 |
| Hagen (1982) | 18,100 | 1,270–38,100 | 44,300 | 3,100–93,000 |
| Costa (1985), $Q_p = f(S * h_d)$ (envelope) | 25,300 | 1,010–30,900 | 55,600 | 2,220–67,800 |
| Costa (1985), $Q_p = f(S)$ | 26,100 | 521–54,700 | 72,200 | 1,440–152,000 |

tained if the failure is initiated at the base of the dam, assumed to be at an elevation of 423.67 m. This produces the maximum amount of head on the developing pipe, and allows it to grow to the largest possible size before the collapse occurs. Table 5 shows summary results of the simulations. For each initial reservoir elevation, a simulation was run with the pipe initiating at an elevation of 423.7 m, and a second simulation was run with the pipe initiating about midway up the height of the dam.

There is a wide variation in the results depending on the assumed initial conditions for the elevation of the seepage failure. The peak outflows and breach widths tend toward the low end of the range of predictions made using the regression equations based on case study data. The predicted failure times are within the range of the previous predictions, and significantly longer than the very short (0.5 to 0.75 h) failure times predicted by the Bureau of Reclamation (1988) equation and the first Von Thun and Gillette equation.

Conclusions

This paper has presented a quantitative analysis of the uncertainty of various regression-based methods for predicting embankment dam breach parameters and peak breach outflows. The uncertainties of predictions of breach width, failure time, and peak outflow

are large for all methods, and thus it may be worthwhile to incorporate uncertainty analysis results into future risk assessment studies when predicting breach parameters using these methods. Predictions of breach width generally have an uncertainty of about $\pm 1/3$ order of magnitude, predictions of failure time have uncertainties approaching ± 1 order of magnitude, and predictions of peak flow have uncertainties of about ± 0.5 to ± 1 order of magnitude, except the Froehlich peak flow equation, which has an uncertainty of about $\pm 1/3$ order of magnitude.

The uncertainty analysis made use of a database of information on the failure of 108 dams compiled from numerous sources in literature (Wahl 1998). Those wishing to make use of this database may obtain it in electronic form (Lotus 1-2-3, Microsoft Excel, and Microsoft Access) on the Internet at http://www.usbr.gov/pmts/hydraulics_lab/twahl/

The case study presented here showed that significant engineering judgment must be exercised in the interpretation of predictions of breach parameters. The results from use of the physically based NWS-BREACH model were reassuring because they fell within the range of values obtained from the regression-based methods. However, at the same time, they also helped to show that even physically based methods can be highly sensitive to the assumptions of the analyst regarding breach morphology and the location of initial breach development. The NWS-BREACH simulations demonstrated the possibility for limiting failure mechanics that were not revealed by the regression-based methods.

Notation

The following symbols are used in this paper:

- B_{avg} = average breach width (m);
- C_b = offset factor in the Von Thun and Gillette breach width equation, varies as a function of reservoir volume;
- \bar{e} = average prediction error;
- e_i = individual prediction errors, log cycles;
- h_b = height of breach (m);
- h_d = height of dam (m);
- h_w = depth of water above breach invert at time of failure (m);

Table 5. Results of National Weather Service-BREACH Simulations of Seepage-Erosion Failures

| Initial water surface elevation (m) | Initial elevation of piping failure (m) | Peak outflow, (m ³ /s) | Time-to-peak outflow, t_p (h) | Breach width at time t_p (m) |
|-------------------------------------|---|-----------------------------------|---------------------------------|--------------------------------|
| Top of joint use | | | | |
| 436.68 | 423.7 | 2,280 | 3.9 | 15.7 |
| 436.68 | 430.1 | 464 | 2.1 | 6.5 |
| Top of flood space | | | | |
| 443.18 | 423.7 | 6,860 | 4.0 | 24.7 |
| 443.18 | 430.1 | 1,484 | 1.4 | 10.3 |

K_o = overtopping multiplier: 1.4 for overtopping; 1.0 for piping;
 MAD = median of absolute deviations from T ;
 Q_p = peak breach outflow (m^3/s);
 S = reservoir storage (m^3);
 S_e = standard deviation of the errors;
 S_{MAD} = estimator of scale derived from the median of the absolute deviations, analogous to standard deviation;
 T = median of the errors, an estimator of location;
 t_f = failure time (h);
 V_{er} = volume of embankment material eroded (m^3);
 V_w = volume of water stored above breach invert at time of failure (m^3);
 \hat{x} = predicted value of parameter;
 x = observed value of parameter; and
 Z_i = standardized error.

References

- Bureau of Reclamation. (1982). *Guidelines for defining inundated areas downstream from Bureau of Reclamation dams*, Reclamation Planning Instruction No. 82-11, U.S. Department of the Interior, Bureau of Reclamation, Denver, 25.
- Bureau of Reclamation. (1988). "Downstream hazard classification guidelines." *ACER Tech. Memorandum No. 11*, U.S. Department of the Interior, Bureau of Reclamation, Denver, 57.
- Costa, J. E. (1985). "Floods from dam failures." U.S. Geological Survey, *Open-File Rep. No. 85-560*, Denver, 54.
- Evans, S. G. (1986). "The maximum discharge of outburst floods caused by the breaching of man-made and natural dams." *Can. Geotech. J.*, 23(4), 385–387.
- Fread, D. L. (1984). *DAMBRK: The NWS dam-break flood forecasting model*, National Weather Service, Office of Hydrology, Silver Spring, Md.
- Fread, D. L. (1988) (revised 1991). *BREACH: An erosion model for earthen dam failures*, National Weather Service, Office of Hydrology, Silver Spring, Md.
- Fread, D. L. (1993). "NWS FLDWAV model: The replacement of DAMBRK for dam-break flood prediction." *Dam Safety '93, Proc., 10th Annual ASDSO Conf.*, Association of State Dam Safety Officials, Lexington, Ky., 177–184.
- Froehlich, D. C. (1987). "Embankment-dam breach parameters." *Hydraulic Engineering, Proc. 1987 ASCE National Conf. on Hydraulic Engineering*, New York, 570–575.
- Froehlich, D. C. (1995a). "Embankment dam breach parameters revisited." *Water Resources Engineering, Proc. 1995 ASCE Conf. on Water Resources Engineering*, New York, 887–891.
- Froehlich, D. C. (1995b). "Peak outflow from breached embankment dam." *J. Water Resour. Plan. Manage. Div., Am. Soc. Civ. Eng.*, 121(1), 90–97.
- Hagen, V. K. (1982). "Re-evaluation of design floods and dam safety." *Proc., 14th Congress of Int. Commission on Large Dams*, International Commission on Large Dams, Paris.
- Hanson, G. J., Cook, K. R., and Temple, D. M. (2002). "Research results of large-scale embankment overtopping breach tests." *2002 ASDSO Annual Conf.*, Association of State Dam Safety Officials, Lexington, Ky.
- Johnson, F. A., and Illes, P. (1976). "A classification of dam failures." *Int. Water Power Dam Constr.*, 28(12), 43–45.
- Kirkpatrick, G. W. (1977). "Evaluation guidelines for spillway adequacy." *The evaluation of dam safety, Engineering Foundation Conf.*, ASCE, New York, 395–414.
- MacDonald, T. C., and Langridge-Monopolis, J. (1984). "Breaching characteristics of dam failures." *J. Hydraul. Eng.*, 110(5), 567–586.
- Rousseeuw, P. J. (1998). "Chapter 17: Robust estimation and identifying outliers." *Handbook of statistical methods for engineers and scientists*, 2nd Ed., H. M. Wadsworth Jr., ed., McGraw-Hill, New York, 17.1–17.15.
- Singh, K. P., and Snorrason, A. (1984). "Sensitivity of outflow peaks and flood stages to the selection of dam breach parameters and simulation models." *J. Hydrol.*, 68, 295–310.
- Soil Conservation Service (SCS). (1981). "Simplified dam-breach routing procedure." *Tech. Release No. 66* (Rev. 1), 39.
- Temple, D. M., and Moore, J. S. (1997). "Headcut advance prediction for earth spillways." *Trans. ASAE*, 40(3), 557–562.
- Von Thun, J. L., and Gillette, D. R. (1990). "Guidance on breach parameters." Internal Memorandum, U.S. Dept. of the Interior, Bureau of Reclamation, Denver, 17.
- Wahl, T. L. (1998). "Prediction of embankment dam breach parameters—A literature review and needs assessment." *Dam Safety Rep. No. DSO-98-004*, U.S. Dept. of the Interior, Bureau of Reclamation, Denver.
- Walder, J. S., and O'Connor, J. E. (1997). "Methods for predicting peak discharge of floods caused by failure of natural and constructed earth dams." *Water Resour. Res.*, 33(10), 12.